

The cancer stem cell potency of group 10-Azadiphosphine metal complexes

XIAO, Zhiyin <<http://orcid.org/0000-0002-1466-0953>>, NORTHCOTE-SMITH, Joshua, JOHNSON, Alice, SINGH, Kuldip and SUNTHARALINGAM, Kogularamanan <<http://orcid.org/0000-0002-7047-6384>>

Available from Sheffield Hallam University Research Archive (SHURA) at:

<https://shura.shu.ac.uk/30641/>

This document is the Published Version [VoR]

Citation:

XIAO, Zhiyin, NORTHCOTE-SMITH, Joshua, JOHNSON, Alice, SINGH, Kuldip and SUNTHARALINGAM, Kogularamanan (2022). The cancer stem cell potency of group 10-Azadiphosphine metal complexes. *European Journal of Inorganic Chemistry*. [Article]

Copyright and re-use policy

See <http://shura.shu.ac.uk/information.html>

The Cancer Stem Cell Potency of Group 10-Azadiphosphine Metal Complexes

Zhiyin Xiao^{+, * [a, b]} Joshua Northcote-Smith^{+, [a]} Alice Johnson,^[a, c] Kuldip Singh,^[a] and Kogularamanan Suntharalingam^{* [a]}

The cancer stem cell (CSC) potency of a series of structurally analogous Group 10-azadiphosphine metal complexes is reported. The complexes comprise a Group 10 metal (Ni for 1, Pd for 2, or Pt for 3), an azadiphosphine ligand, and two chloride ligands. The complexes exhibit micromolar potency towards bulk breast cancer cells and breast CSCs cultured in monolayer systems. The cytotoxicity of the complexes is comparable to or better than clinically used metallopharmaceuticals, cisplatin and carboplatin, and the gold-standard anti-breast CSC agent,

salinomycin. Notably, the breast CSC mammosphere inhibitory effect and potency of the complexes is dependent on the Group 10 metal present, increasing in the following order: $3 < 2 < 1$. This study highlights the importance of the metal within a given series of structurally related compounds to their breast CSC mammosphere activity and reinforces the therapeutic potential of Group 10 coordination complexes as anti-CSC agents.

Introduction

Metal complexes are a vital component of modern cancer treatments.^[1] The platinum(II)-based agents, cisplatin, carboplatin, and oxaliplatin, and the arsenic(III)-based agent, arsenic trioxide are routinely used worldwide by oncologists to treat various forms of cancer.^[2] There are also a handful of other metal-containing compounds that are clinically used to treat specific types of cancers in specific territories, such as nedaplatin (Japan), heptaplatin (Korea), and lobaplatin (China).^[2a] Unfortunately, the current crop of metal-based anticancer agents have distinct disadvantages that translate to non-optimal patient outcomes.^[3] For instance, some types of cancer are inherently resistant against clinically used metal complexes, and other types of cancer acquire resistance through somatic evolution.^[4] Patients receiving metal complexes can also suffer from side effects, ranging from minor to

dose-limiting toxicity.^[5] Germane to relapse and metastasis, the leading cause of cancer associated deaths, clinically employed metal complexes are unable to remove cancer stem cells (CSCs) at their clinically administered doses.^[6] CSCs are sub-populations within tumours that have been heavily linked to tumour regeneration and spread, due to their innate ability to self-renew and differentiate.^[7] The aptitude of CSCs to survive current chemotherapeutic regimens (including metal complexes) stems from their relatively slow cell cycle profiles.^[8] While chemotherapeutics tend to target and kill proliferating cancer cells, they are less effective against slowly dividing cells like CSCs.^[9] In the quest to uncover metal complexes that can remove CSCs at clinically applicable doses and thereby ensure durable outcomes, we and others have prepared, characterised, and conducted preclinical studies on hundreds of metal complexes over the last eight to nine years.^[10] Despite these endeavours, only a handful of metal complexes have shown promising CSC activities *in vitro* and *in vivo* and none have entered clinical trials in humans.^[10b]

The systematic development of structurally analogous metal complexes and the evaluation of their anti-CSC properties with respect to the metal present could greatly benefit and extend the scope of the metallopharmaceutical field. A comprehensive understanding of the anti-CSC properties of related metal complexes, where their structures only differ by the metal present, is missing. This is fundamentally because metal complexes, with metals belonging to the same group, that have been tested in CSC systems thus far, differ markedly in their chemical structures.^[10] This makes comparisons based on the metal present (and its position within a particular group in the periodic table) extremely challenging. We recently reported the anti-breast CSC properties of a series of cationic Group 10-bis(azadiphosphine) complexes.^[11] The complexes differed only by the identity of the metal centre, allowing valid comparisons of their anti-breast CSC activity in the context of the Group 10 metal present. This study indicated that, for Group 10-

[a] Dr. Z. Xiao,⁺ J. Northcote-Smith,⁺ Dr. A. Johnson, Dr. K. Singh, Dr. K. Suntharalingam
School of Chemistry
University of Leicester
Leicester LE1 7RH, UK
E-mail: zhiyin.xiao@zjxu.edu.cn
k.suntharalingam@leicester.ac.uk

[b] Dr. Z. Xiao⁺
College of Biological, Chemical Sciences and Engineering
Jiaxing University
Jiaxing 314001, China

[c] Dr. A. Johnson
Biomolecular Sciences Research Centre
Sheffield Hallam University
Sheffield S1 1WB, UK

[⁺] These authors contributed equally to this work

Supporting information for this article is available on the WWW under <https://doi.org/10.1002/ejic.202200427>

© 2022 The Authors. European Journal of Inorganic Chemistry published by Wiley-VCH GmbH. This is an open access article under the terms of the Creative Commons Attribution License, which permits use, distribution and reproduction in any medium, provided the original work is properly cited.

bis(azadiphosphine) complexes, CSC mammosphere potency was dependent on the Group 10 metal present, increasing 'down the group' in the following order: Ni < Pd < Pt.^[11] Here we have sought to expand this knowledge space by comparing the anti-breast CSC properties of neutral nickel(II), palladium(II), and platinum(II) complexes with a single azadiphosphine ligand and two chloride ligands, **1–3** (Figure 1A). The azadiphosphine ligand was used as it can form stable coordination complexes with Group 10 metals via the formation of strong metal-phosphorus bonds. The azadiphosphine ligand used in the study features a hexyl hydrocarbon chain to endow reasonable hydrophilicity and thus facilitate breast CSC uptake. As the structures of **1–3** only differ by the Group 10 metal present, trends in their breast CSC activity can be rationalised in terms of the identity of the metal.

Results and Discussion

Synthesis and characterisation of Group 10-azadiphosphine metal complexes

The Group 10-azadiphosphine metal complexes **1–3** were prepared as outlined in Figure 1A. The azadiphosphine ligand, **L**¹ was prepared using a previously reported protocol.^[11] The complexes **1–3** were synthesised by reacting **L**¹ with one equivalent of the appropriate Group 10 metal salt (NiCl₂·6H₂O for **1**, Pd(1,5-cyclooctadiene)Cl₂ for **2**, and Pt(1,5-cyclooctadiene)Cl₂ for **3**) in DCM:MeOH or DCM. The complexes **1–3** were isolated in high yields (93–96%) as red (**1**), yellow (**2**) or white (**3**) solids and characterised by ¹H, ¹³C{¹H}, and ³¹P{¹H} NMR, UV-vis spectroscopy and elemental analysis (see ESI, Figures S1–S10). Attachment of **L**¹ (via the phosphorus atoms) to the Group 10 metal centre in **1–3** was confirmed by the large upfield shift of the ³¹P{¹H} NMR signal from 62.13 ppm

(in free **L**¹) to 17.03–41.71 ppm (in **1–3**) (Figure 1B). Single crystals of **3** suitable for X-ray diffraction studies were obtained by layer-diffusion of hexane into a DCM solution of **3** (CCDC 2179559, Figure 1C and Table S1). Selected bond distances and bond angles are presented in Table S2. The structure of **3** consists of platinum(II) bound to two phosphorus atoms belonging to **L**¹, and two chloride ligands. The average P–Pt–P, P–Pt–Cl, and Cl–Pt–Cl angles suggest that **3** adopts a pseudo square-planar structure. The average Pt–P (2.21 Å) and Pt–Cl (2.35 Å) bond distances are consistent with bond parameters for a related platinum(II) complex.^[12]

Lipophilicity and solution stability studies

The lipophilicity of **1–3** was experimentally investigated by measuring the extent to which the complexes partitioned between octanol and water, *P*. The Log*P* values obtained for **1–3** varied from -0.03 ± 0.02 to 0.79 ± 0.01 (Table S3). The amphiphilic nature of **1–3** suggests that the complexes should be reasonably soluble in aqueous solutions necessary for cell-based studies and taken up by dividing cells in reasonable quantities to effect a cytotoxic response. Time course ³¹P{¹H} NMR spectroscopy studies were carried out to assess the stability of **1–3** in solution. The ³¹P{¹H} NMR spectra for **1–3** (10 mM) in DMSO-*d*₆ at 37 °C displayed a single signal throughout the course of 72 h (at 53.29 ppm for **1**, 28.20 ppm for **2**, and 14.25 ppm for **3**) corresponding to the intact complexes (Figures S11–S13). Similar studies in D₂O:DMSO-*d*₆ (5:1) (1 mM) showed a single signal for intact **2** and **3** before and after incubation at 37 °C for 72 h, indicative of good stability (Figures S14–S15). For **1**, the peak associated to the intact complex was present before and after incubation at 37 °C for 72 h, however there was also some evidence for the formation of the oxidised analogues of **L**¹ (assigned based on our previous studies with azadiphosphine ligands) (Figure S16).^[11] Taken together the ³¹P{¹H} NMR studies suggests that the Group 10-azadiphosphine metal complexes are reasonably stable in solution over a 72 h period.

Monolayer cytotoxicity studies

To determine the potency of the Group 10-azadiphosphine metal complexes **1–3** toward bulk breast cancer cells (HMLER) and breast CSC-enriched cells (HMLER-shEcad) grown in monolayer cultures, the MTT assay was used. The IC₅₀ values (concentration required to reduce cell viability by 50%) were interpolated from dose-response curves (Figures S17–S19) and are summarised in Table 1. The complexes **1–3** exhibited micromolar toxicity towards both HMLER and HMLER-shEcad cells. The nickel(II) complex **1** displayed 3-fold higher potency ($p < 0.05$, $n = 18$) toward bulk breast cancer cells than the palladium(II) and platinum(II) complexes **2** and **3**, while the potency of **1–3** toward breast CSCs did not vary significantly. Notably the complexes **1–3** were up to 3-fold and 42-fold more potent towards HMLER-shEcad cells than cisplatin and carbopla-

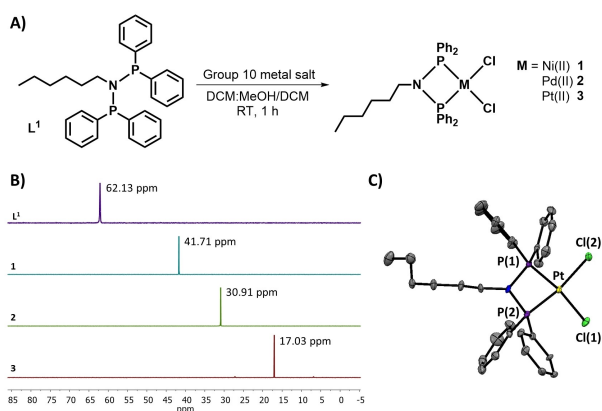


Figure 1. (A) Chemical reaction to form the Group 10-azadiphosphine complexes **1–3** using the azadiphosphine ligand, **L**¹ and the appropriate Group 10 metal salt. (B) ³¹P{¹H} NMR spectra of **L**¹ and **1–3** in CDCl₃. (C) X-ray structure of **3** comprising of one **L**¹ unit and two chloride ligands. Thermal ellipsoids are drawn at 50% probability. C atoms are shown in grey, N in blue, P in purple, Cl in green, and Pt in yellow. The hydrogen atoms have been omitted for clarity.

Compound	HMLER IC ₅₀ [μM] ^[a]	HMLER-shEcad IC ₅₀ [μM] ^[a]	Mammosphere IC ₅₀ [μM] ^[b]
1	1.00 ± 0.01	1.73 ± 0.06	7.54 ± 0.16
2	3.39 ± 0.02	2.86 ± 0.11	9.40 ± 0.07
3	3.05 ± 0.12	2.37 ± 0.26	23.70 ± 0.28
cisplatin ^[c]	2.57 ± 0.02	5.65 ± 0.30	13.50 ± 2.34
carboplatin ^[c]	67.31 ± 2.80	72.39 ± 7.99	18.06 ± 0.40
salinomycin ^[c]	11.43 ± 0.42	4.23 ± 0.35	18.50 ± 1.50

[a] Determined after 72 h incubation (mean of three independent experiments ± SD). [b] Determined after 120 h incubation (mean of three independent experiments ± SD). [c] Reported in references 13, 14, and 17.

tin, respectively.^[13] The complexes 1–3 also displayed comparable toxicity to salinomycin (a leading, clinically tested anti-breast CSC agent) for HMLER-shEcad cells.^[14] Overall, the potency of 1–3 towards bulk breast cancer cells and breast CSCs was similar to previously reported anti-breast CSC metal complexes such as copper(II)-non-steroidal anti-inflammatory drug (NSAID) complexes bearing polypyridyl or Schiff base ligands, a cationic palladium(II)-terpyridine complex with a saccharinate anion, iridium(III) complexes with charged polypyridyl ligands, nickel(II)-NSAID or -dithiocarbamate complexes, and a chiral nickel(II)-supramolecular cylindrical complex.^[10c] Notably, manganese(II)-NSAID complexes with polypyridyl ligands and cobalt(III)-cyclam complexes appended to NSAIDs were significantly more potent towards breast CSCs than 1–3.^[10c]

As a measure of therapeutic potential, the cytotoxicity of 1–3 towards embryonic kidney HEK 293 cells was determined. The complexes 1–3 were significantly less potent ($p < 0.05$, $n = 18$) toward HEK 293 cells (Figure S20 and Table S4) than HMLER and HMLER-shEcad cells, indicating selective toxicity for bulk breast cancer cells and breast CSCs over non-tumorigenic cells.

Mammosphere inhibition and viability studies

Given the promising potencies observed for the Group 10-azadiphosphine metal complexes 1–3 toward breast CSCs cultured in monolayer systems, we investigated their ability to inhibit the formation and viability of three-dimensionally cultured breast CSC mammospheres. Mammospheres are collections of free-floating breast CSCs that provide a more realistic model of tumours than standard monolayer systems given their three-dimensional nature and ability to account for cell-cell adhesion interactions and varying oxygen levels in tissues.^[15]

Treatment of single cell suspensions of HMLER-shEcad cells with 1 and 2 at a non-lethal dose (0.5 μM, determined from monolayer cytotoxicity studies) significantly ($p < 0.05$) reduced the number of mammospheres formed after 5 days incubation (Figure 2A). Addition of the platinum(II) complex 3 (0.5 μM) to single cell suspensions of HMLER-shEcad cells did not lead to a statistically significant ($p = 0.29$) decrease in the number of mammospheres formed after 5 days incubation (Figure 2A).

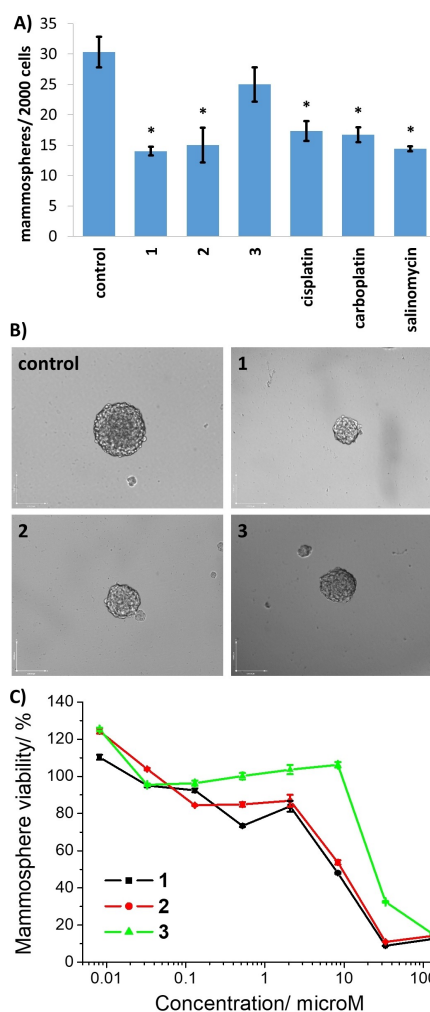


Figure 2. (A) Quantification of mammosphere formation with HMLER-shEcad cells untreated and treated with 1–3, cisplatin, carboplatin, and salinomycin at 0.5 μM after 5 days incubation. Error bars = SD and Student *t*-test, $* = p < 0.05$. (B) Representative bright-field images (x 10) of the mammospheres in the absence and presence of 1–3 (0.5 μM) after 5 day incubation. (C) Representative dose-response curves for the treatment of HMLER-shEcad mammospheres with 1–3 after 5 days incubation.

Under these conditions all of the complexes 1–3 decreased the size of the mammospheres formed, with the nickel(II) complex inducing the greatest reduction in mammosphere size (Figure 2B). Overall, the mammosphere inhibitory effect (according to the number and size of mammospheres formed) increased in the following order: $3 < 2 < 1$. This suggests that the mammosphere inhibitory effect of 1–3 is connected to the Group 10 metal present. Interestingly, the opposite trend was observed for the previously reported Group 10-bis(azadiphosphine) complexes, where the corresponding platinum(II) complex displayed the highest inhibitory effect within the series.^[11] Notably the mammosphere inhibitory effect of the nickel(II) and palladium(II) complexes 1 and 2 was comparable to the effect induced by cisplatin, carboplatin, and salinomycin (0.5 μM for 5 days) (Figure 2A–B and Figure S21). We have previously shown that the addition of the free azadiphosphine ligand L¹ (at 133 μM for 5 days) did not affect mammosphere formation

(in terms of number or size).^[11] Therefore, we can deduce that the Group 10 metal in 1–3 plays a determinant role in their mammosphere inhibitory effect.

The ability of the Group 10-azadiphosphine metal complexes 1–3 to affect mammosphere viability (metabolic activity) was determined using the colorimetric resazurin-based reagent, TOX8. TOX8 has been previously proven to be a suitable reagent for determining tumour spheroid viability as it is able to penetrate multicellular and multilayer systems unlike most other dyes used to assess cell viability.^[16] The IC_{50} values (the concentration required to reduce mammosphere viability by 50%) were interpolated from dose-response curves (Figure 2C) and are summarised in Table 1. The metal complexes 1–3 displayed micromolar potency towards mammospheres, and similarly to the mammosphere formation inhibitory data, the mammosphere potency of 1–3 was dependent on the Group 10 metal. The mammosphere potency increased in the following order: 3 (IC_{50} value = $23.70 \pm 0.28 \mu M$) < 2 (IC_{50} value = $9.40 \pm 0.07 \mu M$) < 1 (IC_{50} value = $7.54 \pm 0.16 \mu M$). The opposite mammosphere cytotoxicity trend was observed for the previously reported Group 10-bis(azadiphosphine) complexes.^[11] The nickel(II) and palladium(II) complexes 1 and 2 displayed significantly ($p < 0.05$) higher potency towards mammospheres than cisplatin, carboplatin, and salinomycin, whereas the platinum(II) complex 3 exhibited lower potency (Table 1).^[13,17] We have previously shown that L^1 was non-toxic towards mammospheres ($IC_{50} > 133 \mu M$).^[11] This implies that the Group 10 metal in 1–3 is a major contributing factor in their mammosphere toxicity.

Conclusion

In summary, we report the synthesis, characterisation, and CSC potency of a family of Group 10 metal complexes 1–3 comprising of an azadiphosphine ligand and two chloride ligands. The attachment of the Group 10 metal (nickel, palladium, or platinum) to the azadiphosphine ligand via the phosphorus atoms was indicated by $^{31}P\{^1H\}$ NMR spectroscopy studies. The pseudo square-planar structure of the platinum(II) complex 3 was shown by X-ray crystallography. The complexes 1–3 were stable in solution over a period of 72 h at a physiologically relevant temperature. The complexes 1–3 displayed similar or better potency towards bulk breast cancer cells and breast CSCs, grown in two-dimensional systems, than cisplatin, carboplatin and salinomycin. Notably, the nickel(II) complex 1 exhibited 2- to 42-fold greater potency for breast CSCs than cisplatin, carboplatin, and salinomycin. Furthermore, 1–3 exhibited up to 6.5-fold greater toxicity towards breast CSCs than non-tumorigenic cells. Mammosphere studies, involving breast CSCs cultured in three-dimensional systems, revealed that the mammosphere inhibitory effect and potency of 1–3 is dependent on the Group 10 metal present. Mammosphere activity increased in the following order: 3 (platinum complex) < 2 (palladium complex) < 1 (nickel complex). Fascinatingly, the previously reported Group 10-bis(azadiphosphine) complexes, with two azadiphosphine ligands, displayed the reverse trend.

In the case of the Group 10-bis(azadiphosphine) complexes, solution stability correlated with CSC mammosphere activity, hence the metal could have largely been playing a role in influencing the structural integrity of the complexes. The complex with the most inert metal, platinum, which formed the most stable complex in solution, displayed the highest CSC mammosphere activity within the Group 10-bis(azadiphosphine) series. For the Group 10-azadiphosphine complexes presented in this study 1–3, the complexes displayed similar solution stabilities therefore the chemical reactivity of the Group 10 metal is more likely to dictate CSC mammosphere activity. As such, within the Group 10-azadiphosphine series 1–3, the complex with the most reactive metal, nickel, displayed the highest CSC mammosphere activity. These results highlight that the nature of the metal present within a given series of coordination compounds could influence their CSC mammosphere activity and that the underlying reason for any differences could be subject to the reactivity of the metal and the structural stability imparted by the metal. The results also highlight the complexities in establishing universal biological activity trends based solely on the metal present (within a given ligand framework). As this study has uncovered Group 10 metal complexes with promising anti-CSC properties, the results provide further motivation for the development of Group 10 metallopharmaceuticals, particularly to target and remove chemoresistant tumour subpopulations like CSCs.

Experimental Section

Materials and Methods. All synthetic procedures were performed under normal atmospheric conditions. UV-vis absorption spectra were recorded on a Cary 3500 UV-Vis spectrophotometer. 1H , $^{13}C\{^1H\}$, and $^{31}P\{^1H\}$ NMR were recorded at room temperature on a Bruker Avance 400 spectrometer (1H 400.0 MHz, ^{13}C 100.6 MHz, ^{31}P 162.0 MHz) with chemical shifts (δ , ppm) reported relative to the solvent peaks of the deuterated solvent. All J values are given in Hz. Elemental analysis of the compounds prepared was performed commercially by the University of Cambridge. $NiCl_2 \cdot 6H_2O$, $Pd(1,5\text{-cyclooctadiene})Cl_2$, and $Pt(1,5\text{-cyclooctadiene})Cl_2$ were purchased from Sigma Aldrich or Alfa Aesar and used without further purification. Solvents were purchased from Fisher and used without further purification. The azadiphosphine ligand, L^1 was synthesised according to our reported protocol.^[11]

Synthesis of $[Ni^{II}(L^1)Cl_2]$, 1. A DCM solution (4 mL) containing L^1 (94 mg, 0.2 mmol) was added to a methanol solution (4 mL) containing $NiCl_2 \cdot 6H_2O$ (48 mg, 0.2 mmol). The reaction mixture was stirred for 1 h at ambient temperature. Upon removal of the solvent under vacuum, the resultant residue was washed with diethyl ether (3 mL \times 2). Solvent-layer diffusion of hexane into a DCM solution containing the washed solid enabled isolation of 1 as a dark-red powder (112 mg, 93%). 1H NMR (400 MHz, $CDCl_3$): δ 7.97 (dd, J = 13.1, 6.8 Hz, 8H, Ar-H), 7.67 (t, J = 7.5 Hz, 4H, Ar-H), 7.55 (t, J = 7.5 Hz, 8H, Ar-H), 2.85–2.70 (m, 2H, CH_2), 1.08–0.92 (m, 4H, $2 \times CH_2$), 0.92–0.82 (m, 2H, CH_2), 0.78 (td, J = 8.5, 1.7 Hz, 2H, CH_2), 0.70 (t, J = 7.2 Hz, 3H, CH_3); $^{13}C\{^1H\}$ NMR (101 MHz, $CDCl_3$): δ 133.50, 133.07, 129.38, 127.59, 48.56, 30.95, 29.52, 26.57, 22.35, 13.86; $^{31}P\{^1H\}$ NMR (162 MHz, $CDCl_3$): δ 41.71; UV-vis (PBS, λ_{max}/nm): 268 (ϵ = 1.4×10^4 Lmol $^{-1}$ cm $^{-1}$), 306 (ϵ = 1.8×10^4 Lmol $^{-1}$ cm $^{-1}$), 336 (ϵ = $8.5 \times$

$10^3 \text{ Lmol}^{-1} \text{ cm}^{-1}$); Anal. Calcd. for $\text{C}_{30}\text{H}_{33}\text{NP}_2\text{Cl}_2\text{Ni}$ (%): C, 60.14; H, 5.55; N, 2.34. Found: C, 60.12; H, 5.32; N, 2.44.

Synthesis of $[\text{Pd}^{\text{II}}(\text{L}^1)\text{Cl}_2]$, 2. A DCM solution (4 mL) containing L^1 (94 mg, 0.2 mmol) was added to a DCM solution (4 mL) containing $\text{Pd}(\text{1,5-cyclooctadiene})\text{Cl}_2$ (58 mg, 0.2 mmol). The reaction mixture was stirred for 1 h at ambient temperature. Upon removal of the solvent under vacuum, the resultant residue was washed with diethyl ether (4 mL \times 3). Solvent-layer diffusion of hexane into a DCM solution containing the washed solid enabled isolation of **2** as a yellow powder (124 mg, 94%). ^1H NMR (400 MHz, CDCl_3): δ 7.94–7.81 (m, 8H, Ar-H), 7.65 (tdd, $J=4.4, 2.6, 1.6$ Hz, 4H, Ar-H), 7.61–7.47 (m, 8H, Ar-H), 3.08–2.91 (m, 2H, CH_2), 1.07 (dt, $J=11.5, 7.7$ Hz, 2H, CH_2), 1.03–0.94 (m, 2H, CH_2), 0.92–0.76 (m, 4H, $2 \times \text{CH}_2$), 0.70 (t, $J=7.2$ Hz, 3H, CH_3); $^{13}\text{C}\{^1\text{H}\}$ NMR (101 MHz, CDCl_3): δ 133.70, 133.53, 129.61, 127.63–126.71, 49.59, 30.92, 29.55, 26.54, 22.32, 13.85; $^{31}\text{P}\{^1\text{H}\}$ NMR (162 MHz, CDCl_3): δ 30.91; UV-vis (PBS, $\lambda_{\text{max}}/\text{nm}$): 265 ($\epsilon=1.2 \times 10^4 \text{ Lmol}^{-1} \text{ cm}^{-1}$), 363 ($\epsilon=8.4 \times 10^3 \text{ Lmol}^{-1} \text{ cm}^{-1}$); Anal. Calcd. for $\text{C}_{30}\text{H}_{33}\text{NP}_2\text{Cl}_2\text{Pd}$ (%): C, 55.70; H, 5.14; N, 2.17. Found: C, 55.49; H, 4.83; N, 2.14.

Synthesis of $[\text{Pt}^{\text{II}}(\text{L}^1)\text{Cl}_2]$, 3. A DCM solution (4 mL) containing L^1 (94 mg, 0.2 mmol) was added to a DCM solution (4 mL) containing $\text{Pt}(\text{1,5-cyclooctadiene})\text{Cl}_2$ (75.2 mg, 0.2 mmol). The reaction mixture was stirred for 1 h at ambient temperature. Upon removal of the solvent under vacuum, the resultant residue was washed with diethyl ether (4 mL \times 3). Solvent-layer diffusion of hexane into a DCM solution containing the washed solid enabled isolation of **3** as a white powder (143 mg, 96%). ^1H NMR (400 MHz, CDCl_3): δ 7.85 (dt, $J=13.6, 4.2$ Hz, 8H, Ar-H), 7.63 (t, $J=7.4$ Hz, 4H, Ar-H), 7.54 (dd, $J=10.9, 4.0$ Hz, 8H, Ar-H), 3.00–2.81 (m, 2H, CH_2), 1.13–0.93 (m, 4H, $2 \times \text{CH}_2$), 0.84 (dddd, $J=20.9, 15.5, 9.8, 5.3$ Hz, 4H, CH_2 , $2 \times \text{CH}_2$), 0.71 (t, $J=7.2$ Hz, 3H, CH_3); $^{13}\text{C}\{^1\text{H}\}$ NMR (101 MHz, CDCl_3): δ 133.52, 133.31, 129.42, 128.02–126.83, 49.98, 30.94, 29.47, 26.54, 22.35, 13.86; $^{31}\text{P}\{^1\text{H}\}$ NMR (162 MHz, CDCl_3): δ 17.03 (t, $J_{\text{P-Pt}}=1648$ Hz); UV-vis (PBS, $\lambda_{\text{max}}/\text{nm}$): 269 ($\epsilon=1.4 \times 10^4 \text{ Lmol}^{-1} \text{ cm}^{-1}$), 314 ($\epsilon=1.1 \times 10^4 \text{ Lmol}^{-1} \text{ cm}^{-1}$); Anal. Calcd. for $\text{C}_{30}\text{H}_{33}\text{NP}_2\text{Cl}_2\text{Pt}$ (%): C, 48.99; H, 4.52; N, 1.90. Found: C, 48.79; H, 4.48; N, 1.91.

X-ray Single Crystal Diffraction Analysis. Single crystals of complex **3** were obtained by layer-diffusion of hexane into a DCM solution of the metal complex. Crystals suitable for X-ray diffraction analysis were selected and mounted on a Bruker Apex 2000 CCD area detector diffractometer using standard procedures. Data was collected using graphite-monochromated Mo- $\text{K}\alpha$ radiation ($\lambda=0.71073$) at 150(2) K. Crystal structures were solved and refined using the Bruker SHELXTL software.^[18] All hydrogen atoms were located by geometrical calculations, and all non-hydrogen atoms were refined anisotropically.

Measurement of the Water-Octanol Partition Coefficient (LogP). The LogP values for **1–3** were determined using the shake-flask method and UV-vis spectroscopy. The 1-octanol used in this experiment was pre-saturated with water. An aqueous solution of **1–3** (500 μL , 100 μM) was incubated with 1-octanol (500 μL) in a 1.5 mL tube. The tube was shaken at room temperature for 24 h. The two phases were separated by centrifugation and the **1–3** content in each phase was determined by UV-vis spectroscopy.

Time Course $^{31}\text{P}\{^1\text{H}\}$ NMR Spectroscopy. The Group 10-azadiphosphine metal complexes **1–3** were dissolved in $\text{DMSO}-d_6$ (10 mM) or $\text{D}_2\text{O}:\text{DMSO}-d_6$ (5:1) (1 mM) and incubated at 37 °C for 72 h. At various time intervals, the $^{31}\text{P}\{^1\text{H}\}$ NMR spectrum of the $\text{DMSO}-d_6$ (10 mM) or $\text{D}_2\text{O}:\text{DMSO}-d_6$ (5:1) (1 mM) solutions was recorded on a Bruker Avance 400 spectrometer (^{31}P 162.0 MHz).

Cell Lines and Cell Culture Conditions. The human mammary epithelial HMLER and HMLER-shEcad cell lines were kindly donated by Prof. R. A. Weinberg (Whitehead Institute, MIT). The human

embryonic kidney HEK 293 cell line was acquired from American Type Culture Collection (ATCC, Manassas, VA, USA). HMLER and HMLER-shEcad cells were maintained in Mammary Epithelial Cell Growth Medium (MEGM) with supplements and growth factors (BPE, hydrocortisone, hEGF, insulin, and gentamicin/amphotericin-B). HEK 293 cells were maintained in Dulbecco's Modified Eagle's Medium (DMEM) supplemented with (non-USA origin) foetal bovine serum (10%) and penicillin/streptomycin (1%). The cells were grown at 310 K in a humidified atmosphere containing 5% CO_2 .

Monolayer Cytotoxicity Studies. Exponentially growing cells were seeded at a density of approximately 5×10^3 cells per well in 96-well flat-bottomed microplates and allowed to attach for 24 h prior to addition of compounds. Various concentrations of the test compounds (0.0004–100 μM) were added and incubated for 72 h at 37 °C (total volume 200 μL). Stock solutions of the compounds were prepared as 10 mM DMSO solutions and diluted using cell media. The final concentration of DMSO in each well was $\leq 1\%$. After 72 h, 20 μL of MTT (4 mg mL^{-1} in PBS) was added to each well and the plates incubated for an additional 4 h at 37 °C. The media/MTT mixture was eliminated and DMSO (100 μL per well) was added to dissolve the formazan precipitates. The optical density was measured at 550 nm using a 96-well multiscanner autoreader. Absorbance values were normalised to (DMSO-containing) control wells and plotted as concentration of test compound versus % cell viability. IC_{50} values were interpolated from the resulting dose dependent curves. The reported IC_{50} values are the average of three independent experiments ($n=18$).

Tumoursphere Formation and Viability Assay. HMLER-shEcad cells (5×10^3) were plated in ultralow-attachment 96-well plates (Corning) and incubated in MEGM supplemented with B27 (Invitrogen), 20 ng mL^{-1} EGF and 4 $\mu\text{g mL}^{-1}$ heparin (Sigma) for 5 days. Studies were also conducted in the presence of **1–3**, cisplatin, carboplatin, and salinomycin (0–133 μM). Mammospheres treated with **1–3**, cisplatin, carboplatin, and salinomycin (0.5 μM for 5 days) were counted and imaged using an inverted microscope. The viability of the mammospheres was determined by addition of a resazurin-based reagent, TOX8 (Sigma). After incubation for 16 h, the fluorescence of the solutions was read at 590 nm ($\lambda_{\text{ex}}=560$ nm). Viable mammospheres reduce the amount of the oxidised TOX8 form (blue) and concurrently increase the amount of the fluorescent TOX8 intermediate (red), indicating the degree of mammosphere cytotoxicity caused by the test compound. Fluorescence values were normalised to DMSO-containing controls and plotted as concentration of test compound versus % mammosphere viability. IC_{50} values were interpolated from the resulting dose dependent curves. The reported IC_{50} values are the average of three independent experiments, each consisting of two replicates per concentration level (overall $n=6$).

Deposition Number 2179559 (for **3**) contains the supplementary crystallographic data for this paper. These data are provided free of charge by the joint Cambridge Crystallographic Data Centre and Fachinformationszentrum Karlsruhe Access Structures service www.ccdc.cam.ac.uk/structures.

Acknowledgements

K.S. is supported by an EPSRC New Investigator Award (EP/S005544/1). Z.X. thanks the National Natural Science Foundation of China (21807047) for financial support.

Conflict of Interest

The authors declare no conflict of interest.

Data Availability Statement

The data that support the findings of this study are available from the corresponding author upon reasonable request.

Keywords: Antitumour agents · Cancer stem cells · Group 10 compounds · Transition metals · Mammosphere studies

- [1] A. Casini, A. Vessi res, S. M. Meier-Menches, *Metal-based Anticancer Agents*, RSC Publishing **2019**.
- [2] a) T. C. Johnstone, K. Suntharalingam, S. J. Lippard, *Chem. Rev.* **2016**, *116*, 3436–3486; b) S. Gibaud, *Metal-based Anticancer Agents*, The Royal Society of Chemistry **2019**, pp. 196–214.
- [3] T. C. Johnstone, G. Y. Park, S. J. Lippard, *Anticancer Res.* **2014**, *34*, 471–476.
- [4] B. A. Chabner, T. G. Roberts Jr., *Nat. Rev. Cancer* **2005**, *5*, 65–72.
- [5] L. Kelland, *Nat. Rev. Cancer* **2007**, *7*, 573–584.
- [6] F. Tomao, A. Papa, L. Rossi, M. Strudel, P. Vici, G. Lo Russo, S. Tomao, *J. Exp. Clin. Cancer Res.* **2013**, *32*, 48.
- [7] a) L. V. Nguyen, R. Vanner, P. Dirks, C. J. Eaves, *Nat. Rev. Cancer* **2012**, *12*, 133–143; b) J. Marx, *Science* **2007**, *317*, 1029–1031.
- [8] a) N. Moore, S. Lyle, *J. Oncol.* **2011**, *2011*; b) L. N. Abdullah, E. K. Chow, *Clin. Transl. Med.* **2013**, *2*, 3.
- [9] M. Dean, T. Fojo, S. Bates, *Nat. Rev. Cancer* **2005**, *5*, 275–284.
- [10] a) K. Laws, K. Suntharalingam, *ChemBioChem* **2018**, *19*, 2246–2253; b) A. Johnson, J. Northcote-Smith, K. Suntharalingam, *Trends Chem.* **2021**, *3*, 47–58; c) Y. Li, B. Liu, H. Shi, Y. Wang, Q. Sun, Q. Zhang, *Dalton Trans.* **2021**, *50*, 14498–14512.
- [11] Z. Xiao, A. Johnson, K. Singh, K. Suntharalingam, *Angew. Chem. Int. Ed.* **2021**, *60*, 6704–6709; *Angew. Chem.* **2021**, *133*, 6778–6783.
- [12] V. Gallo, P. Mastroianni, C. F. Nobile, P. Braunstein, U. Englert, *Dalton Trans.* **2006**, *19*, 2342–2349.
- [13] A. Eskandari, A. Kundu, S. Ghosh, K. Suntharalingam, *Angew. Chem. Int. Ed.* **2019**, *58*, 12059–12064; *Angew. Chem.* **2019**, *131*, 12187–12192.
- [14] J. N. Boodram, I. J. McGregor, P. M. Bruno, P. B. Cressey, M. T. Hemann, K. Suntharalingam, *Angew. Chem. Int. Ed.* **2016**, *55*, 2845–2850; *Angew. Chem.* **2016**, *128*, 2895–2900.
- [15] G. Dontu, W. M. Abdallah, J. M. Foley, K. W. Jackson, M. F. Clarke, M. J. Kawamura, M. S. Wicha, *Genes Dev.* **2003**, *17*, 1253–1270.
- [16] R. Mezencev, L. Wang, J. F. McDonald, *J. Ovarian Res.* **2012**, *5*, 30.
- [17] C. Lu, K. Laws, A. Eskandari, K. Suntharalingam, *Dalton Trans.* **2017**, *46*, 12785–12789.
- [18] G. Sheldrick, *Acta Crystallogr.* **2008**, *A64*, 112–122.

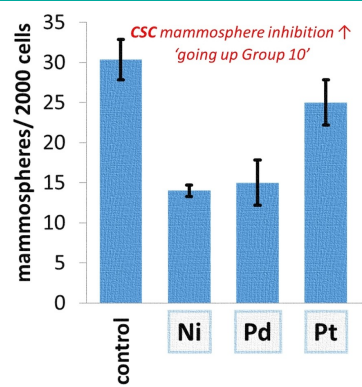
Manuscript received: July 4, 2022

Revised manuscript received: August 1, 2022

Accepted manuscript online: August 3, 2022

RESEARCH ARTICLE

A handful of metal complexes are used to treat cancer patients however they are all unable to remove relapse-causing cancer stem cells (CSCs). Here we compare the breast CSC mammosphere inhibitory effect and potency of a series of Group 10-azadiphosphine metal complexes. Our results show that the Group 10 metal significantly influences breast CSC mammosphere activity.



Dr. Z. Xiao*, J. Northcote-Smith, Dr. A. Johnson, Dr. K. Singh, Dr. K. Suntharalingam*

1 – 7

The Cancer Stem Cell Potency of Group 10-Azadiphosphine Metal Complexes

